



Load Tracking Enhancement of a Grid
Connected SOFC System Using an Advanced
Controller in Real Time.

Preeti Gupta, Vivek Pahwa and Yajvender Pal Verma

EasyChair preprints are intended for rapid dissemination of research results and are integrated with the rest of EasyChair.

February 26, 2020

Load tracking enhancement of a grid connected SOFC system using an advanced controller in real time

Preeti Gupta*

Research Scholar, EEE
University Institute of Engineering
& Technology, Panjab University,
Chandigarh, India
er.guptapreeti07@gmail.com

Vivek Pahwa

Assistant Professor, EEE
University Institute of Engineering
& Technology, Panjab University,
Chandigarh, India

Y. P. Verma

Associate Professor, EEE
University Institute of Engineering
& Technology, Panjab University,
Chandigarh, India

Abstract- Modeling, measurement and control are the most important aspects, for making any renewable source to be in synchronism at the earliest with the utility grid during any load demand power change. This is to put minimum stress at the grid during load change as per the latest grid-code. Therefore, in this paper an efficient and rugged active power controller based on ANFIS has been implemented for improving the load tracking of grid connected static renewable source i.e. SOFC. Additionally, this controller is subjected to the constraint that the fuel utilization factor of the SOFC should stay within safe limits. The comparison of this proposed controller shows superior performance in contrast to conventional integral controller. The results have been verified in real time environment provided by OPAL-RT's simulator through hardware-in-loop.

Index Terms- ANFIS; grid synchronisation; HIL; load-tracking; OPAL-RT; real-time; SIL; SOFC;

I. INTRODUCTION

With growing industrialization, form of power generation has changed from the past few decades [1]. Earlier the common forms were heat, nuclear or thermal and now the trend has shifted towards cleaner forms of energies like solar, wind, chemical, hydro, etc. These newer forms of power generation are renewable, non-polluting and efficient with abundant availability [2], [3]. Among these forms of energies, renewable chemical energy has recently gained popularity, for instance solid oxide fuel cell (SOFC) which converts chemical to electrical energy [4]–[6]. This power source alone is not sustainable until connected to the AC utility grid. But, this grid connected source which is static, slow and DC power generator creates serious problems like synchronization and poor load power sharing with grid during any load demand power change in contrast to conventional grid connected AC generator [7]. The researcher in [8] has attempted to synchronize DC source using inverter with its associated control circuitry and phase locked loop (PLL), but still there is a scope for further improvement. In [9] and [10] researchers have tried to investigate the load tracking with conventional controllers like PI and optimal PI. Other approaches like fuzzy and adaptive fuzzy logic based controllers in [11], [12] respectively have also been used to fast the load tracking under rugged conditions, still these controllers are quite slow. One of the most popular and adaptive controller is ANFIS (adaptive neural fuzzy inference system) which has self learning ability with unified rules [13]–[16]. It is efficient and has been applied in number of applications of power system [17]–[19].

While tracking the load demand power change, fuel cell follows inverter or visa-versa at a slower pace because inverter is a fast acting device and operates within fractions of seconds. On the other hand, SOFC is a slow acting device and takes few seconds to reach the steady state. This creates a lag between active power demand and supply [20], [21]. Another important aspect is that if more power is fetched from SOFC to cover-up this demand and supply lag then, there is a possibility that SOFC's life is greatly affected. Since the net loss in the system is generally kept minimal in order to improve the load tracking capability, but especially in case of SOFC the load tracking is a critical factor because the power generation depend on its chemical reaction that takes time to occur to generate requisite amount of power. Thus apart from reduction in overall losses in the power circuit of the system, it is important to fasten the rate at which the fuel is utilized, known as process of fuel utilization in the system in order to reduce the time taken by SOFC in response to any change in active power demand [22], [23]. This is maintained by keeping the utilization factor within limits i.e. 0.7 to 0.9 in order to ensure the safe operation of grid connected SOFC system while improving the load tracking capability [24].

With the above mentioned issues, the need for adoption of an advanced controller to address the problem of gap between power demand and supply in a grid connected SOFC system while maintaining the grid synchronization and life of SOFC is necessitated. In [25] effort has been made to fill this gap for a stand-alone SOFC system using a fuzzy predictive control approach. However, the validation is completed using simulation study under certain constraints but still it lacks in providing the robust design of a controller to be directly implanted on an actual system. Since real time implementation is the need of modernization because the controllers designed with real time conditions are easily implemented onto the actual power system [26], [27]. Thus, many real time simulators like OPAL-RT, RTDS, dSPACE etc are available that provide features for the analysis of the power system in real time [28]–[31]. Among these OPAL-RT's ARTEMIS-SSN real time simulator has been utilised in this research work as it provides a platform through a software, real time laboratory (RT-LAB) where the test system model is prepared. This simulator provides two ways for model execution in real time, (1) software-in-loop (SIL) and (2) hardware-in-loop (HIL). In SIL the model is prepared and executed for safety and then finally implemented in HIL. In this way, the validation of the work as per real conditions is done in a secure manner. It also ensures the robust and accurate solutions of the work within prescribed time frame [32], [33].

In this present work, an advanced ANFIS based active power controller has been implemented on a grid connected SOFC system in real time to synchronize it with the utility grid at the earliest as well as to improve the dynamic performance of the SOFC by keeping its utilization factor within safe limits.

The work in this paper is organized in sections as, section-II presents the configuration and modeling of the system, section-III discusses the active power controller, its advancements and real time implementation are discussed in section-IV and V respectively, in the next section discussion is elaborated on the results obtained using the proposed controller in real time and finally in the last section conclusions are drawn.

II. SYSTEM CONFIGURATION AND MODELLING

The system under investigation consists of a grid connected SOFC system as shown in figure 1. This section elaborates the detailed discussion on each of the components of the system below:

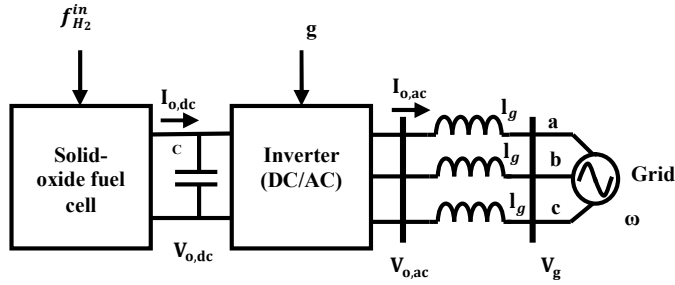


Fig. 1 A grid connected SOFC system

A. SOFC and its control

It generates electrical energy from chemical energy through thermal and electrochemical processes [34]–[36]. The chemical reaction occurs when hydrogen (H_2) and oxygen (O_2) in air combines to form water some electrons are released which travel from anode to cathode. Thus, these released electrons participate to generated DC power is given in (1).

$$P_{o,dc} = V_{o,dc} I_{o,sofc} \quad (1)$$

where, $I_{o,sofc}$ and $V_{o,dc}$ are produced SOFC dc current and voltage respectively. The SOFC voltage is calculated using Nernst equation given in (2)

$$V_{o,dc} = V_0^o + \frac{RT}{4F} \ln \left[\frac{(p_{H_2})^2 p_{O_2}}{(p_{H_2O})^2} \right] - r I_{o,sofc} \quad (2)$$

where, $V_0^o = V_0^o + k_E(T - 298)$ is reaction free voltage which depends on the standard potential of the cell (V_0^o) and its operating temperature (T); R is the gas constant; F is faraday constant and p_{H_2} , p_{O_2} & p_{H_2O} are the effective partial pressures of H_2 , O_2 and H_2O gas; r is an equivalent resistive loss component of the cell.

The fuel input ($f_{H_2}^{in}$) to SOFC are mainly hydrogen molecules which are acquired through a fuel controller. This $f_{H_2}^{in}$ is basically a fuel flow rate of H_2 gas (kmol/second) in SOFC. Generally, the fuel processing takes huge amount of time which makes SOFC a slow

acting device for any load change. Thus, the fuel controller reduces the fuel processing time and stimulate SOFCs dynamic response [20]. During any load change, it is important to bound the performance variables of SOFC to stay within limits to secure the life of SOFC [21]. Hence the boundaries are formed in terms of mainly three terms, (1) operating temperature (T) from 1173K to 1273K, (2) produced active power ($P_{o,dc}$) within 0.1 to 1 per unit and, (3) the rate at which the fuel is utilized in SOFC in the range 0.7 to 0.9 respectively [22]. The fuel utilization rate also known as utilisation factor, U_f shown in figure 2.

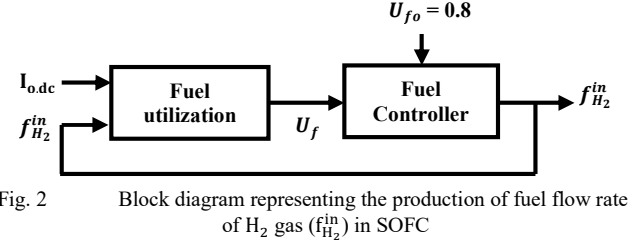


Fig. 2 Block diagram representing the production of fuel flow rate of H_2 gas ($f_{H_2}^{in}$) in SOFC

In this figure, fuel utilisation factor is obtained using (3) which is further fed to the fuel controller.

$$U_f = \frac{2k_r I_{o,sofc}}{f_{H_2}^{in}} \quad (3)$$

where, k_r is chemical reaction constant.

B. Inverter and its control

Inverter is used to convert DC to AC in order to provide sustainability through grid connection. The output DC power is assumed equal as AC power under steady state operation as a result the instantaneous power developed across the inverter is given in (4)

$$P_{o,ac} = 1.5(V_{o,acd} I_{o,acd} + V_{o,acq} I_{o,acq}) \quad (3)$$

where, $V_{o,acd}$, $V_{o,acq}$ are dq-axis voltages and $I_{o,acd}$, $I_{o,acq}$ are dq-axis currents on AC-side of inverter.

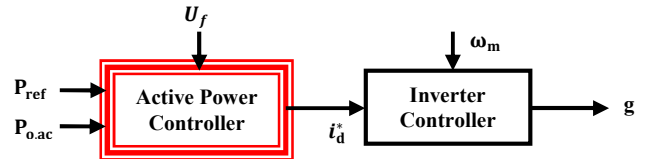


Fig. 3 Block diagram of gate pulse (g) generation for inverter

The inverter receives gate pulses, g through inverter controller as shown in the figure 3. This controller utilizes ω_m the angular frequency of the PLL and i_d^* the output of active power controller (discussed in later section) to generate the required gate pulses.

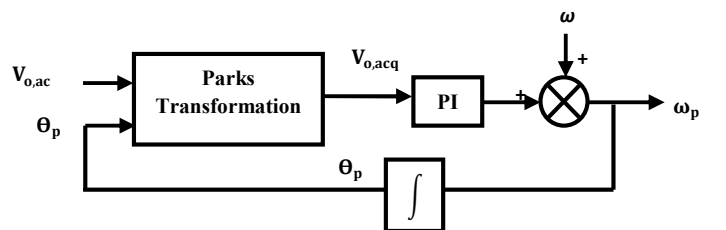


Fig. 4 Block diagram of PLL modelling

C. Phase locked loop (PLL)

The modelling of PLL is given in (5)

$$\dot{\omega}_m = k_p V_{o,acq} + k_i V_{o,acq} \quad (4)$$

where, k_p , k_i are the proportional and integral constants respectively. With the help of PLL the angle, Θ_g is also calculated which is required for the transformation from 'dq0' to 'abc' and vice-versa.

D. Grid synchronisation

The grid is working at angular frequency $\omega = 2\pi f$ where f is the rated frequency of the system. The dynamic equations on AC and DC side of the inverter are given in (6)

$$\begin{aligned} l_g \dot{I}_{o,acd} &= V_{o,acd} - \cos\delta V_g + \omega_m l_g I_{o,acq} \\ l_g \dot{I}_{o,acq} &= V_{o,acq} + \sin\delta V_g - \omega_m l_g I_{o,acd} \\ V_{o,dc} &= \frac{1}{C} (I_{sofc} - I_{o,dc}) \end{aligned} \quad (6)$$

where, l_g is grid tied inductance, $\omega_m = 2\pi f_m$, δ is the load angle, C is the DC link capacitor and $I_{o,dc}$ is the DC side current.

When a step load change is applied onto the grid connected SOFC system, it follows the reference power, P_{ref} as given in (7)

$$J \dot{\omega}_m = P_\varepsilon - D(\omega_m - \omega) \quad (7)$$

where, $P_\varepsilon = P_{ref} - P_{o,ac}$; $J = -\frac{1.5}{k_i} i_{gq} (1 - k_p l_g I_{o,acd})$; $D = -\frac{1.5}{k_i} k_p I_{o,acq} V_{o,ac} \cos\delta$; J and D are the equivalent moment of inertia and damping factor of the grid connected SOFC system respectively. The equation given in (7) can be understood in two ways i.e. during steady-state and during transient period.

During steady-state period, ω_m is constant therefore, the rate of change of ω_m w.r.t. time, t is zero as a result the right hand term in (7) becomes zero. Also, the equivalent damping factor, D is zero therefore, P_ε also becomes zero. In other words, the frequency of PLL, ω_m and grid frequency ω are equal during steady-state period. On the other hand during transient period, due to change in load demand power, ω_m is not constant. Hence, the derivative of ω_m is also not zero. Now, the swing equation in (7) is balanced by J . This J has been developed by PLL and its associated control circuitry given earlier. It is important to keep this J positive and $(\omega_m - \omega)$ almost zero in order to maintain stable grid synchronization otherwise active power imbalance occurs in the system.

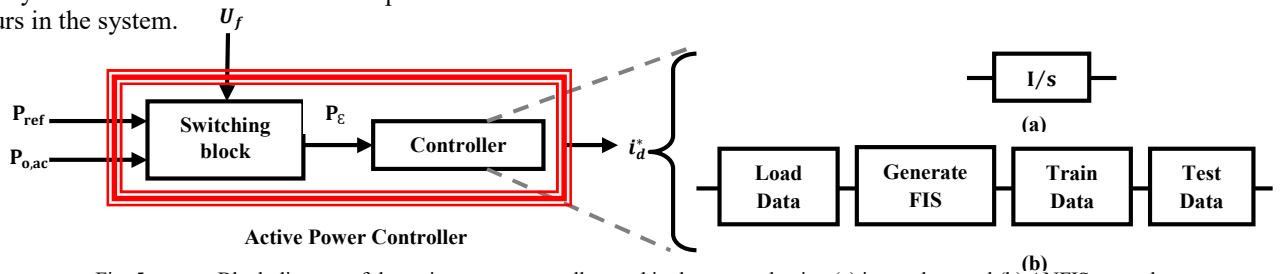


Fig. 5 Block diagram of the active power controller used in the system having (a) integral control (b) ANFIS control

III. ACTIVE POWER CONTROLLER

To maintain grid synchronization and overcome the gap between demand and supply in a grid connected SOFC system, an active power controller is applied. It regulates the change in active power (P_ε) to maintain the two important conditions for successful operation of grid connected SOFC system as: (1) $0.7 \leq U_f \leq 0.9$ and (2) $\omega_m - \omega = 0$. Thus, this controller helps in generating improved change in active power (P_ε^*) by fulfilling the above two conditions as given in (8)

$$P_\varepsilon^* = P_{ref} - P_{o,ac}^* \quad (8)$$

where, $P_{o,ac}^* = \begin{cases} 0.7P_{o,ac} & \forall U_f < 0.7 \\ 0.9P_{o,ac} & \forall U_f > 0.9 \\ P_{o,ac} & \forall 0.7 \leq U_f \leq 0.9 \end{cases}$ is the adjusted output power of SOFC when operated under constant temperature. It is obtained using a switching block that defines the boundary limits of utilization factor as shown in figure 5. It can be seen that when the fuel utilization factor is within safe boundaries the exact output active demand power is referred to the inverter, whereas in other cases reduced value is referred in order to keep fuel cell within secured life limits.

Next, it is mandatory to maintain grid synchronism, thus a balance is created through an integral controller to nullify P_ε^* as shown in (9)

$$P_\varepsilon^* = k_{ei} (\omega_m - \omega_n) \quad (9)$$

where, k_{ei} is the integral constant and ω_n is the nominal frequency of the system.

IV. ADVANCED ACTIVE POWER CONTROLLER

To address the two issues of grid connected SOFC system as mentioned in previous section, artificial intelligent based controller i.e. ANFIS with a switching block has been adopted. It is an adaptive multi-layer network that combines the characteristics of fuzzy inference systems (FIS) with features of artificial neural networks (ANN). It is a toolbox in MATLAB/ SIMULINK which optimizes the objective as per the training. Thus, it constructs an adaptive network based on fuzzy rules and membership functions to improve the performance of the system. It provides speedy operation with accuracy and learning ability of membership functions [37]–[40]. The design and implementation of the ANFIS-controller involves basic four steps given in figure 5 (b). Since it is well established controller thus, the discussion is restricted on its implementation only. The controlled output generated using ANFIS is depicted with the help of the controlled surface and rule viewer as shown in figure 6 (a) and (b) respectively.

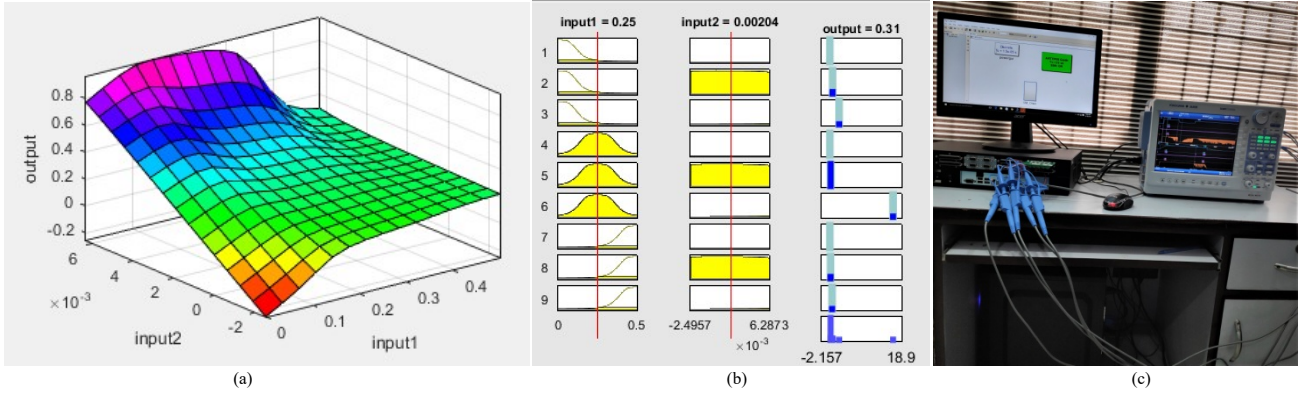


Fig. 6 (a) The control surface of ANFIS, (b) Rule viewer of ANFIS and (c) The experimental set-up of test model in HIL

V. REAL TIME ENVIRONMENT

To validate the performance of an advanced active power controller based on ANFIS, OPAL-RT's real time simulator, OP4510 is utilised. It is composed of Intel processors and FPGAs [41], [42]. It utilises RT-LAB software for model preparation and the execution is performed in two ways i.e. software-in-loop (SIL) and hardware-in-loop (HIL). The SIL involves basic five steps i.e. model preparation, compilation, building, loading and execution whereas HIL involves additional sixth step i.e. monitoring.

The real time execution produces results instantly as .mat file in SIL and on the external display device like DSO in HIL. The results obtained in HIL are transferred via DB37-connector to DSO by scaling the signals in the range of -16 to 16 volts as shown in the figure 6 (c). The signals transmitted from the simulator to DSO correspond to 1division = 1volt and one volt correspond to 0.1 p.u. for active powers (P_o and P_{ref}), 15Hz for frequencies (f and f_m) and 0.1 for utilization factor (U_f) respectively. With the help of the corresponding vaules, the gains are introduced while transmitting the voltage signals to DSO for safe and observable operation in laboratory.

VI. RESULTS AND DISCUSSION

In this work, the SOFC as shown in figure 1 has power capacity of 100kW and it is operating at constant temperature of 1273K with 450 number of series cells in a stack which have a base voltage of 530 volts (1.18X450). This SOFC is connected to a grid of 440 volts at 60Hz supply frequency through an IGBT/Diodes based inverter. Here, the dynamic response of this system has been discussed using an advanced controller based on ANFIS. This controller is implemented on a real time experimental set-up as shown in figure 6c provided by OPAL-RT's ARTEMIS simulator.

The system is subjected to three varying step load demand power changes of 100% increase and 50% both decrease and increase for analysing the ruggedness of the developed controller. The total simulation time considered for the system execution is 100 seconds with both integral and ANFIS control mechanisms used in active power controller. The results of all the variables with integral controller are represented with black lines whereas ANFIS based results are coloured for each type of the variable as green, blue, pink, violet and orange representing $P_{o,ac}^*$, P_{ref} ,

f , f_m and U_f respectively. The discussion proceeds with the results obtained in two environments i.e. SIL and HIL as shown in figures 7 and 8 respectively.

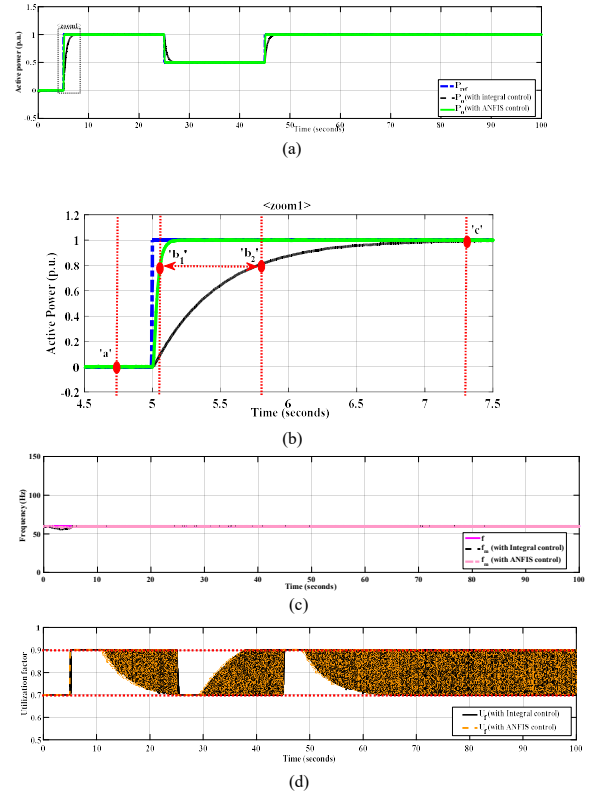


Fig. 7 Response of SOFC system with (black lines) and ANFIS (coloured lines) based active power controller in SIL

The comparative analysis of both the active powers shown in figure 7a in SIL environment reveals that when load is changed from 0% to 100% at 5second, the system with proposed controller quickly follows the reference power in contrast to integral active power controller. Similar trend is observed during next two 50% load demand power changes. This showcases the superior performance of the proposed controller.

Further major observation can be understood from the zoomed view of figure 7a i.e. figure 7b as:

- During steady-state period i.e. at operating points 'a' and 'c' the frequency of PLL and grid are equal i.e. $\omega_m = \omega$ and $P_{\xi}^* = 0$ with both the controllers.
- During transient period i.e. at operating point 'b₁' and 'b₂' due to step load demand power change,

$\omega_m \neq \omega$ and $P_E^* \neq 0$. This instability has been controlled by both the controllers but the proposed controller has shows faster tracking mechanism.

Next, the difference between reference power, P_{ref} and power produced by SOFC system, $P_{o,ac}$ is being fulfilled by grid. Analysis of power response in figure 7a also reveals that due to the improved performance of proposed controller, the share of grid power has been reduced in contrast to integral controller.

In figure 7c the frequency graph shows that the system frequency is unaffected even during severe power change of 100% with both the controllers. It shows the rigidity of the SOFC based system with the utility grid.

Apart from synchronization, another objective was to keep the SOFC within its safe limit during transient as well as during steady-state period i.e. utilization factor has to be maintained between 0.7 to 0.9. This is important to maintain the life of the SOFC intact. It can be observed from the SIL results of U_f that during complete time span it remains within mentioned safe boundaries. This is achieved with the help of the switching block incorporated with active power controller discussed in section 2.

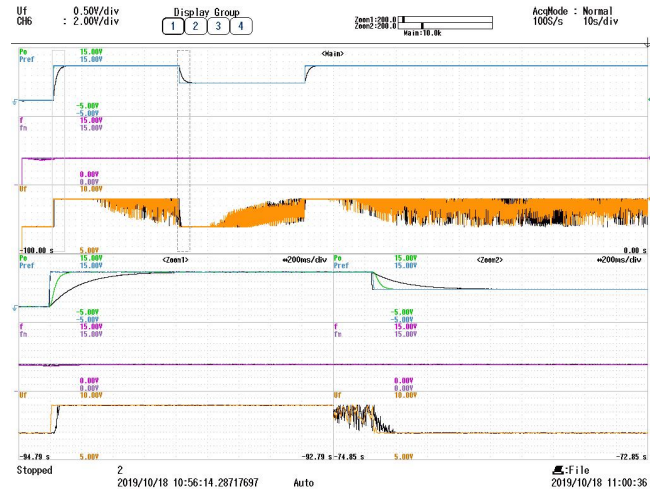


Fig. 8 Response of SOFC system with Integral (black lines) and ANFIS (coloured lines) based active power controller in HIL

In HIL environment, the performance of the developed controller is validated by OPAL-RT's real time simulator as shown in figure 8.

VII. CONCLUSION

In this work, apart from systematically achieving the main objectives i.e. improved synchronization of grid connected SOFC system while keeping the utilization factor of SOFC within safe range of 0.7 to 0.9. This rugged ANFIS based active power controller is being compared to conventional integral based controller for a load demand power change of 100% and 50%. It is concluded that the transient performance of SOFC has improved from 4-5 seconds (integral control) to 0.2-0.3 seconds (ANFIS control). Thus, an appreciable reduction of share of active power from grid has been observed.

Additionally, one step ahead stage has been developed for the researcher for its ready implementation because the whole system has been developed in real time environment considering the real time conditions using HIL with

precision and accuracy. In future this work can be extended using other advanced controllers based on symbiotic organisms search optimization, whale optimization algorithm and grey wolf optimization [43]-[45].

VIII. ACKNOWLEDGMENT

The authors are thankful to MHRD, Government of India for giving the grant to UIET, Panjab University Chandigarh for Design Innovation Centre vide letter no.17-11/2015-PN.1 under which the work has been carried out.

References

- [1] P. Denholm, E. Ela, B. Kirby, and M. Milligan, "The Role of Energy Storage with Renewable Electricity Generation," Colorado, 2010.
- [2] M. S. Mahmoud, N. M. Alyazidi, and M. I. Abouheaf, "Adaptive intelligent techniques for microgrid control systems: A survey," *Int. J. Electr. Power Energy Syst.*, vol. 90, pp. 292–305, 2017.
- [3] M. Moafi, M. Marzband, M. Savaghebi, and J. M. Guerrero, "Energy management system based on fuzzy fractional order PID controller for transient stability improvement in microgrids with energy storage," *Int. Trans. Electr. Energy Syst.*, vol. 26, no. 10, pp. 2087–2106, 2016.
- [4] P. Costamagna, A. De Giorgi, L. Magistri, G. Moser, L. Pellaco, and A. Trucco, "A Classification Approach for Model-Based Fault Diagnosis in Power Generation Systems Based on Solid Oxide Fuel Cells," *IEEE Trans. Energy Convers.*, vol. 31, no. 2, pp. 676–687, 2016.
- [5] J. Milewski, M. Wołowicz, and J. Lewandowski, "Comparison of SOE/SOFC system configurations for a peak hydrogen power plant," *Int. J. Hydrogen Energy*, vol. 42, no. 5, pp. 3498–3509, 2017.
- [6] P. Sarmah and T. K. Gogoi, "Performance comparison of SOFC integrated combined power systems with three different bottoming steam turbine cycles," *Energy Convers. Manag.*, vol. 132, pp. 91–101, 2017.
- [7] N. H. Behling, *Fuel Cells: Current Technology Challenges and Future Research Needs*. Newnes, 2012.
- [8] J. Liu *et al.*, "Impact of Power Grid Strength and PLL Parameters on Stability of Grid-Connected DFIG Wind Farm," *IEEE Trans. Sustain. Energy*, vol. 3029, no. c, pp. 1–12, 2019.
- [9] G. Wu, K. Y. Lee, and W. Yang, "Modeling and Control of Power Conditioning System for Grid-connected Fuel Cell Power Plant," in *National Science Foundation under grant ECCS*, 2013.
- [10] S. A. Taher and S. Mansouri, "Optimal PI controller design for active power in grid-connected SOFC DG system," *Electr. Power Energy Syst.*, vol. 60, pp. 268–274, 2014.
- [11] K. Chatterjee, R. Shankar, and A. Kumar, "Fuzzy Logic Based Controller for a Grid-Connected Solid Oxide Fuel Cell Power Plant," *J. Fuel Cell Sci. Technol.*, vol. 11, pp. 1–9, 2014.
- [12] N. Chanasut and S. Premrudeepreechacharn, "Maximum Power Control of Grid-Connected Solid Oxide Fuel Cell System Using Adaptive Fuzzy Logic Controller," in *IEEE Industry Applications Society Annual Meeting*, 2008, pp. 1–6.
- [13] C. T. Krasopoulos, M. E. Beniakar, and A. G. Kladas, "Multi-Criteria PM Motor Design based on ANFIS evaluation of EV Driving Cycle Efficiency," *IEEE Trans. Transp. Electr.*, vol. 7782, no. c, pp. 1–1, 2018.
- [14] J. Saroha, M. Singh, and D. K. Jain, "ANFIS based add-on controller for unbalance voltage compensation in low voltage microgrid," *IEEE Trans. Ind. Informatics*, 2018.
- [15] U. Sowmmiya and G. Uma, "ANFIS-based sensor fault-tolerant

- control for hybrid grid,” *IET Gener. Transm. Distrib.*, vol. 12, no. 1, pp. 31–41, 2018.
- [16] J. Wu, H. Wu, Y. Song, T. Zhang, J. Zhang, and Y. Cheng, “Adaptive Neuro-fuzzy inference system based estimation of EAMA elevation joint error compensation,” *Fusion Eng. Des.*, vol. 126, pp. 170–173, 2018.
- [17] G. S. Kumar, B. K. Kumar, and M. K. Mishra, “Mitigation of voltage sags with phase jumps by UPQC with PSO-Based ANFIS,” *IEEE Trans. Power Deliv.*, vol. 26, no. 4, pp. 2761–2773, 2011.
- [18] J. P. S. Catalão, H. M. I. Pousinho, and V. M. F. Mendes, “Hybrid Wavelet-PSO-ANFIS Approach for Short-Term Electricity Prices Forecasting,” *IEEE Trans. Power Syst.*, vol. 26, no. 1, pp. 137–144, 2011.
- [19] Y. K. Semero, J. Zhang, and D. Zheng, “PV power forecasting using an integrated GA-PSO-ANFIS approach and Gaussian process regression based feature selection strategy,” *CSEE J. Power Energy Syst.*, vol. 4, no. 2, pp. 210–218, 2018.
- [20] L. Sun, G. Wu, Y. Xue, J. Shen, D. Li, and K. Y. Lee, “Coordinated Control Strategies for SOFC Power Plant in a Microgrid,” *IEEE Trans. Energy Convers.*, vol. 33, no. 1, pp. 1–9, 2018.
- [21] Y. H. Li, S. S. Choi, and S. Rajakaruna, “An analysis of the control and operation of a solid oxide fuel-cell power plant in an isolated system,” *IEEE Trans. Energy Convers.*, vol. 20, no. 2, pp. 381–387, 2005.
- [22] Y. Li, Q. Wu, and H. Zhu, “Hierarchical Load Tracking Control of a Grid-Connected Solid Oxide Fuel Cell for Maximum Electrical Efficiency Operation,” *Energies*, vol. 8, no. 3, pp. 1896–1916, Mar. 2015.
- [23] S. Han, L. Sun, J. Shen, L. Pan, and K. Lee, “Optimal Load-Tracking Operation of Grid-Connected Solid Oxide Fuel Cells through Set Point Scheduling and Combined L1-MPC Control,” *Energies*, vol. 11, no. 4, p. 801, Mar. 2018.
- [24] J. H. Yi and T. S. Kim, “Effects of fuel utilization on performance of SOFC/gas turbine combined power generation systems,” *J. Mech. Sci. Technol.*, vol. 31, no. 6, pp. 3091–3100, 2017.
- [25] Tiejun Zhang and Gang Feng, “Rapid Load Following of an SOFC Power System via Stable Fuzzy Predictive Tracking Controller,” *IEEE Trans. Fuzzy Syst.*, vol. 17, no. 2, pp. 357–371, Apr. 2009.
- [26] B. K. Bose, “An Adaptive Hysteresis-Band Current Control Technique of a Voltage-Fed PWM Inverter for Machine Drive System,” *IEEE Trans. Ind. Electron.*, vol. 37, no. 5, pp. 402–408, 1990.
- [27] A. Bellini, S. Bifaretti, and S. Costantini, “A new approach to hysteresis modulation techniques for NPC inverters,” in *IEEE International Symposium on Industrial Electronics ISIE-02*, 2002, pp. 844–849.
- [28] Y. Li, D. M. Vilathgamuwa, and P. C. Loh, “Design, Analysis, and Real-Time Testing of a Controller for Multibus Microgrid System,” *IEEE Trans. Power Electron.*, vol. 19, no. 5, pp. 1195–1204, Sep. 2004.
- [29] A. Rubaai, A. R. Ofoli, and D. Cobbinah, “DSP-based real-time implementation of a hybrid H-infinity adaptive fuzzy tracking controller for servo-motor drives,” *IEEE Trans. Ind. Appl.*, vol. 43, no. 2, pp. 476–484, 2007.
- [30] X. Guillaud *et al.*, “Applications of Real-Time Simulation Technologies in Power and Energy Systems,” *IEEE Power Energy Technol. Syst. J.*, vol. 2, no. 3, pp. 103–115, 2015.
- [31] E. Breaz, F. Gao, D. Paire, and R. Timovan, “Fuel cell modeling With dSPACE and OPAL-RT real time platforms,” in *IEEE Transportation Electrification Conference and Expo (ITEC)*, 2014, pp. 1–6.
- [32] X. Fu, S. Mouhamadou Seye, J. Mahseredjian, M. Cai, and C. Dufour, “A Comparison of Numerical Integration Methods and Discontinuity Treatment for EMT Simulations,” in *2018 Power Systems Computation Conference (PSCC)*, 2018, no. 2, pp. 1–7.
- [33] G. M. Jonsdottir, M. S. Almas, M. Baudette, M. P. Palsson, and L. Vanfretti, “RT-SIL performance analysis of synchrophasor-and-active load-based power system damping controllers,” in *IEEE Power & Energy Society General Meeting*, 2015, pp. 1–5.
- [34] P. Costamagna, P. Costa, and V. Antonucci, “Micro-modelling of solid oxide fuel cell electrodes,” *Electrochim. Acta*, vol. 43, no. 3–4, pp. 375–394, 1998.
- [35] A. Bertei, J. Mertens, and C. Nicolella, “Electrochemical simulation of planar solid oxide fuel cells with detailed microstructural modeling,” *Electrochim. Acta*, vol. 146, pp. 151–163, 2014.
- [36] A. Gebregergis, P. Pillay, D. Bhattacharyya, and R. Rengaswamy, “Solid Oxide Fuel Cell Modeling,” *IEEE Trans. Ind. Electron.*, vol. 56, no. 1, pp. 139–148, 2009.
- [37] H. R. Baghaee, M. Mirsalim, G. B. Gharehpetian, H. A. Talebi, and A. Niknam-Kumle, “A Hybrid ANFIS/ABC-based Online Selective Harmonic Elimination Switching Pattern for Cascaded Multi-level Inverters of Microgrids,” *IEEE Trans. Ind. Electron.*, pp. 1–1.
- [38] H. Turabieh, M. Mafarja, and S. Mirjalili, “Dynamic Adaptive Network-Based Fuzzy Inference System (D-ANFIS) for the imputation of missing data for Internet of Medical Things Applications,” *IEEE Internet Things J.*, vol. XX, no. X, pp. 1–1.
- [39] M. Gheisarnejad, P. Karimaghaee, J. Boudjadar, and M.-H. Khooban, “Real-time Cellular Wireless Sensor Testbed for Frequency Regulation in Smart Grids,” *IEEE Sens. J.*, vol. 1748, no. c, pp. 1–10, 2019.
- [40] H. R. Baghaee, M. Mirsalim, G. B. Gharehpetian, H. A. Talebi, and A. Niknam-Kumle, “Notice of Violation of IEEE Publication Principles: A Hybrid ANFIS/ABC-based Online Selective Harmonic Elimination Switching Pattern for Cascaded Multi-level Inverters of Microgrids,” *IEEE Trans. Ind. Electron.*, pp. 1–11, 2019.
- [41] J. Blanger, P. Venne, and J.-N. Paquin, “The What, Where and Why of Real-Time Simulation,” *IEEE PES Gen. Meet.*, pp. 37–49, 2010.
- [42] C. Dufour and J. Belanger, “A PC-Based Real-Time Parallel Simulator of Electric Systems and Drives,” in *International Conference on Parallel Computing in Electrical Engineering*, 2005, pp. 105–113.
- [43] N. S. Rathore, V. P. Singh, and B. D. H. Phuc, “A modified controller design based on symbiotic organisms search optimization for desalination system”, in *Journal of Water Supply: Research and Technology – AQUA*, vol. 68, No. 5, pp. 337-345, 2019.
- [44] N. S. Rathore, and V. P. Singh, “Whale Optimization Algorithm Based Controller Design for Reverse Osmosis Desalination Plants”, in *International Journal of Intelligent Engineering Informatics*, 2018.
- [45] N. S. Rathore, V. P. Singh, B. Kumar, “Controller Design for DOHA Water Treatment Plant using Grey Wolf Optimization”, in *Journal of Intelligent and Fuzzy Systems*, vol. 35, No. 5, pp. 5329-5336, 2018.